Chin. J. Geochem. (2015) 34(2):194–200
DOI 10.1007/s11631-015-0039-5

ORIGINAL ARTICLE

An experimental determination of W, Nb, and Ta partition coefficients between P-rich peraluminous granitic melt and coexisting aqueous fluid

Yong Tang · Hui Zhang

Received: 9 September 2014 / Revised: 2 December 2014 / Accepted: 5 December 2014 / Published online: 6 February 2015

Abstract The partition coefficients of W, Nb, and Ta between the P-rich peraluminous granitic melt and the coexisting aqueous fluid were determined at 800–850 °C and 0.5–1.5 kbar. The experimental results showed that the partition coefficients D_W, D_{Nb}, and D_{Ta} ($D_i^{v/m} = C_i^v/C_i^m$, where C_i^v and C_i^m denote the concentrations of an element, i, in the aqueous fluid and the melt, respectively) were less than 0.1. All partition coefficients were affected by pressure, but there was no evidence for the complexation of P_2O_5 with these elements in the granitic melt or aqueous fluid, except for with W in the fluid. The results showed that W, Nb, and Ta tended to partition into the granitic melt and, in the late period of crystallization of P-rich magma, they formed independent minerals.

Keywords Partition coefficient · P-rich granitic melt · Fluid

1 Introduction

Some peraluminous granites, pegmatites, and rhyolites—particularly those with S-type affinity—are enriched in phosphorus. Whole-rock values of >1 wt% P_2O_5 have been reported for certain granites (Raimbault et al. 1995; Lentz 1997; London 1998; Raimbault and Burol 1998; Zhang 2001). Extremely high concentrations of phosphorus in evolved granitic melts lead to the crystallization of amblygonite-montebrasite $LiAlPO_4$(F,OH), ithiophylite-triphylite Li(Mn,Fe)PO_4 (London 1987), and/or ferromagnesian phosphate minerals including childernite-eosphorite series phases and sarcopside (London et al. 1999). Although the effect of phosphorus on the viscosity of granitic melts and the solubility of water in granitic melts appears to be small, compared with F or B (Dingwell et al. 1993; Holtz et al. 1993; Toplis and Dingwell 1996), experimental studies have shown that phosphorus can lower the solidus temperatures of granitic melts and can expand the liquidus field of quartz, ultimately leading to the formation of peralkaline, silicate-poor residual melts (Wyllie and Tuttle 1964; London et al. 1993). Rare-element ore deposits mineralized with W, Nb, and Ta are closely associated with the P-rich peraluminous igneous rocks spatially and temporally (e.g., Baxiannao tungsten deposit, Yichun 414 Nb–Ta deposit, Nanping No. 3 pegmatite, and Beauvoir granite) (Huang et al. 2002; Li et al. 2010; Raimbault et al. 1995; Yang et al. 1994), but the effect of phosphorus on the vapor/melt partitioning behavior of W, Nb and Ta is still not known in detail. The purpose of this study is to investigate the partitioning of these elements and phosphorus's role in the partitioning of these ore metals in magmatic-hydrothermal systems.

Y. Tang · H. Zhang (✉)
Laboratory for High Temperature and High Pressure Study of the Earth's Interior, Institute of Geochemistry, Chinese Academy of Sciences, 46 Guanshui Road, Guiyang 550002, Guizhou, People's Republic of China
e-mail: zhanghui@vip.gyig.ac.cn

Y. Tang
e-mail: tangyong@vip.gyig.ac.cn

2 Experimental methods

2.1 Starting materials

An albite granite, termed YS-02-48 from the Yichun 414 pluton, was the starting material (Table 1). A small block of the albite granite was cleaned in distilled water, dried, then ground in an agate mortar until it was less than 200 mesh in grain size. To meet the analytical accuracy

Table 1 Compositions of the sample and starting glass versus Macusanite and Ongonite (wt%)

Sample	YS-02-48	Macusanite[a]	Ongonite[a]	P0T	P2T	P5T	P8T
SiO_2	73.82	72.32	72.47	74.16	72.86	70.79	68.06
TiO_2	0.02	0.02	0.00	0.02	0.02	0.02	0.01
Al_2O_3	15.17	15.63	16.66	15.56	15.21	14.75	14.39
Fe_2O_3	0.32	0.52[b]	0.52[b]	0.41	0.40	0.40	0.41
MnO	0.09	0.06	0.11	0.09	0.09	0.09	0.09
MgO	0.02	0.00	0.25	0.19	0.2	0.19	0.44
CaO	0.49	0.23	0.18	0.33	0.33	0.32	0.43
Na_2O	5.12	4.10	4.65	5.24	5.13	4.97	4.95
K_2O	3.42	3.53	3.13	3.61	3.52	3.40	3.28
P_2O_5	0.32	0.58	/	0.27	1.91	4.83	7.71
F	0.23	1.31	1.09	/	/	/	/
B_2O_3	0.02	0.62	/	/	/	/	/
H_2O	0.74	0.30	0.98	/	/	/	/
total	99.69	99.78	100.43	99.87	99.66	99.74	99.75
ASI	1.17	1.42	1.47	1.19	1.18	1.19	1.16
W[b]				428	485	505	541
Nb[b]				221	229	278	423
Ta[b]				198	216	202	247

[a] Datas from London et al. (1989)

[b] The total Fe as FeO, / not determined (these elements are in ppm)

requirements of trace elements in experimentally run-products, glass and aqueous fluid by LA-ICPMS and solution ICP-MS, certain concentrations, e.g., 500 ppm W, 200 ppm Nb and, 200 ppm Ta, together with various concentrations of phosphorus, were doped in the initial material during the glasses preparation by using a silicon–molybdenum electric furnace. Phosphorus in the initial glass was added in the form of $(NH_4)H_2PO_4$, and trace elements were added in the forms of corresponding oxides.

Analytically pure powders of (NH_4) H_2PO_4, trace element oxides and albite granite powder were mixed by grinding them in an agate mortar for at least 4 h. The mixtures were fused in a platinum crucible in a silicon–molybdenum electric furnace (JGMT-5/180 type) at 1500 °C; fusion time was limited to 1 h to minimize alkali loss, and the melts were quenched in water. In order to generate homogeneous glasses, this process of grinding, fusing, and rapid quenching, was repeated 3 to 4 times for each starting composition. Finally, the glasses were ground to <50 μm for use in experiments. The compositions of the glasses were analyzed by XRF and are shown in Table 1.

2.2 Experimental procedure

All runs were conducted in cold-seal Rapid Quenching pressure Vessels (RQV, a kind of "externally heated cold-seal pressure vessel"), using water as the pressure medium for durations of 144 h. The run temperature and pressure were measured by a WRPK-103 type platinum–rhodium thermocouple and Bourdon-tube pressure gauge with errors of 1 °C and 0.05 kbar, respectively. The maximum temperature gradient at 1 kbar was 5 °C over the 5-cm long capsule, as determined by the calibration of the temperature profile of the tubular electric furnace. The oxygen fugacity (fO_2) of the experimental charge was not directly controlled. The use of GH220 vessels (commensurate to René-41, composed of a Ni-based alloy), coupled with the thermal dissociation of the water pressure medium $(2H_2O = 2H_2 + O_2)$ in the vessel, imposes a hydrogen fugacity (by the establishment of osmotic equilibrium between the charge and the pressure buffer within 24 h) equal to the nickel–nickel oxide (NNO) solid-state oxygen fugacity buffer on the experimental charge (Chou 1987; Simon et al. 2005).

About 200 mg of starting glass was loaded into gold capsules, which were 4-mm in outer diameter, 3.8-mm in inner diameter and 50-mm in length. About 200 μl of deionized water was injected into the capsule slowly by using a micro-injector to keep the solid–liquid ratio of 1:1. The loaded capsule was immersed in ice water and welded shut by oxy-acetylene flame. The sealed capsule was placed in an oven at 110 °C overnight. After checking for leakage and making sure of no change in mass (<0.5 mg), the capsule was placed inside the cold-seal rapid quenched vessel (RQV), which was inserted into a horizontal tubular electric furnace. The charge was pressurized with water to 0.5 kbar, and then heated to 850 °C in 2–3 h. Then, the pressure was adjusted to the final run pressure of 1.0 kbar. After melting the charge at 850 °C for 24 h, the run temperature was dropped at a rate of 1 °C/min to 800 °C, where the charge was kept for 144 h, in a state that was sufficient to make partitioning experiments in this work

attain equilibrium. At the end of the experiment, the pressure vessel was withdrawn from the tubular heating electric furnace and tilted upwards (at 90° angle from the horizontal). The gold capsule slid into the quenching part of vessel and was then quenched isobarically from 800 °C to ambient-temperature in less than 10 s.

The capsule was removed from the vessel, cleaned with distilled water, examined microscopically and weighed, in order to determine whether the capsule had remained sealed during the run. Only those capsules that showed mechanical integrity and mass loss (<0.5 mg) were processed for analysis. After centrifugation for 30 min, the top end of the capsule was pierced with a stainless steel needle, and the solution was extracted using a syringe. Then the capsule was dried, opened by a razor blade, and boiled in hydrochloric acid for 30 min. After the acid treatment, the sample was rinsed several times with de-ionized water. All of the solutions obtained during these operations were added to the solution withdrawn from the capsule, and then diluted to 5 ml in preparation for analysis. The purpose of the acid treatment is to re-dissolve material precipitated from the fluid during quenching. In this process, the glass does not appear to be significantly affected (Keppler and Wyllie 1991). The quenched silicate melt formed clear, colorless and translucent glass. Sub-microscopic cavities, formed by vapor bubbles, were observed in the appearance of glass. The total volume of these bubbles is estimated at <0.1 vol% of the fluid.

2.3 Analysis of experimental products

Chemical composition of the initial glasses was determined by XRF at the State Key Laboratory of Ore Deposit Geochemistry, Institute of Geochemistry, Chinese Academy of Sciences. The major-element composition of the run-product glasses was analyzed by the Shimadzu EMPA-1600 electron microprobe with wavelength dispersive spectrometry (WDS) at the State Key Laboratory of Ore Deposit Geochemistry, Institute of Geochemistry, Chinese Academy of Sciences. Natural Macusite glass was used as standards for the major element, except P, and synthesized P-bearing glass (P_2O_5 wt% = 2) was used as a standard for P. In order to reduce the loss of alkalies during analysis, the analytical conditions for Na, Al, K and Si were at 20-kV acceleration potential, 2-nA beam current and a 20-μm defocused spot. For other major elements the conditions were at 20 kV acceleration potential, 20-nA beam current and a 20-μm defocused spot (Morgan and London 1996, 2005). The counting time for all elements was 30 s.

The trace-element concentration in the glasses was measured by LA-ICP-MS (Agilent 7500 Series) at the State Key Laboratory of Continental Dynamics, Northwestern University, Xi'an. It was equipped with a Elan 600DRC quadrupole mass spectrometer and a 193-nm ArF excimer laser (Geolas200 M laser ablation system). Spots that were petrographically devoid of vapor bubbles were chosen for ablation, and the diameter of the laser ablation beam was set to 30 μm. Analysis methods and operating conditions were defined in detail previously (Gao et al. 2002). A US National Institute of Standards and Technology (NIST) standard reference material, NBS-610, was used as the reference silicate glass, and the concentration of Si, determined by EMPA, was used as an internal standard for the quantification of the rare-element concentration in the glasses.

The trace-element concentrations of the aqueous fluids were measured using the solution ICP-MS (Elan 600) at the Isotope Laboratory of Institute of Guangzhou Geochemistry, Chinese Academy of Sciences. Indium (10 bbp in standard solutions) was used as the internal standard for the quantification of REE concentration in the aqueous fluid. According to a number of determined results of standard samples, the relative error of LA-ICP-MS and solution ICP-MS were both less than 10 %.

2.4 Sources of experimental error

Much of the error of the partition coefficients comes from the analyses of both the glass and aqueous phases. This error is small if the partition coefficient is less than unity (?) Keppler and Wyllie (1991). With the ICP-MS and LA-ICPMS analyses, the analytical uncertainty is generally <10 %. D_i represents the ratio of two analyses, so the uncertainty in D_i is <14 %.

3 Experimental results and discussions

3.1 The major compositions

It has been determined that the liquidus of the studied initial magmatic systems, which contains 5 wt% H_2O, ranges from 810 °C at 0.27 wt% P_2O_5 to 740 °C at 7.71 wt% P_2O_5, under a pressure of 1.0 kbar (Tang et al. 2009). The 1:1 ratio of the solid–liquid in the experimental charges makes the experimental systems H_2O-oversatured. Thus, it is reasonable to consider that there are only melt and fluid phases in the experimental phase equilibrium systems at 1.0 kbar and 800 °C.

Compared with the corresponding initial glasses (P0T, P2T, P5T and P8T) (Table 1), the main chemical compositions of the run-product glasses (Table 2) have lower content of SiO_2, Al_2O_3, Na_2O and K_2O, and no variation of the Fe–Mg components. Microprobe analytical totals for the run-product glasses are in the range of 89.78–94.78 wt%, implying that about 5.22–10.22 wt%

Table 2 Average chemical compositions of the run-product glasses (melts), determined by EMPA (in wt%)

Sample	P0T				P2T				P5T				P8T			
No	30–1	27–7	26–7	28–3	30–7	24–8	23–8	28–4	29–1	24–7	26–4	28–7	30–8	26–3	26–8	28–8
P (kbar)	0.5	1	1	1.5	0.5	1	1	1.5	0.5	1	1	1.5	0.5	1	1	1.5
T (°C)	850	800	850	800	850	800	850	800	850	800	850	800	850	800	850	800
SiO_2	70.55	69.13	68.09	67.79	69.42	66.20	67.35	66.17	66.19	64.98	65.07	66.02	64.14	65.14	64.46	62.36
Al_2O_3	15.51	14.71	14.95	15.60	14.28	14.58	14.95	14.75	14.24	14.36	14.80	14.34	14.31	14.31	14.39	14.26
Na_2O	4.19	4.00	3.95	3.61	4.13	3.30	3.72	3.58	4.04	3.78	3.88	3.53	3.50	3.50	3.55	3.31
K_2O	3.56	3.25	3.38	3.18	3.12	3.06	3.13	3.22	2.86	2.98	2.81	2.81	2.73	2.73	2.80	2.73
FeO	0.54	0.37	0.50	0.52	0.29	0.32	0.32	0.33	0.28	0.34	0.33	0.35	0.33	0.33	0.34	0.34
MgO	0.08	0.06	0.17	0.16	0.10	0.09	0.12	0.12	0.08	0.17	0.10	0.09	0.11	0.11	0.11	0.10
MnO	0.09	0.07	0.07	0.07	0.06	0.07	0.06	0.06	0.06	0.07	0.06	0.06	0.06	0.06	0.07	0.06
CaO	0.09	0.36	0.40	0.30	0.28	0.25	0.29	0.26	0.16	0.21	0.12	0.01	0.20	0.20	0.33	0.45
TiO_2	0.01	0.01	0.01	0.01	0.01	0.01	0.01	0.01	0.00	0.01	0.01	0.01	0.01	0.01	0.01	0.01
P_2O_5	0.17	0.18	0.23	0.20	1.42	1.38	1.34	1.28	3.34	3.68	3.50	3.40	6.19	6.09	6.01	6.20
Total	94.78	92.14	91.76	91.44	93.12	89.25	91.28	89.78	91.24	90.57	90.68	90.63	91.58	92.48	92.07	89.82
ASI	1.43	1.37	1.38	1.57	1.35	1.59	1.50	1.51	1.42	1.46	1.54	1.62	1.58	1.58	1.52	1.56

H_2O was dissolved in the melts. The significant increase of the ASI (Al-saturation index, ASI = $Al_2O_3/(Na_2O + K_2O + CaO)$ in mole) indicates that melt-fluid interactions result in more Na, K and Ca partitioning into the fluid phase than Al.

Based on trace element concentrations and masses of the initial, run-product glasses and fluid phase, as well as taking into account 4 wt% solubility of peraluminous melt in aqueous fluid (Webster 1990) and different H_2O solubility in different run-product glasses (5.22–10.22 wt%), the recovery of trace element can be estimated to be from 85.9 to 98.6 % in all of the runs. The high recovery states that our experimental results in this paper are reliable.

3.2 Tungsten

Experimental data for the partitioning of tungsten is shown in Fig. 1 and Table 3. The partition coefficients of tungsten vary from 0.003 to 0.07. According to our experimental results, tungsten fractionates toward the melt.

Phosphate, as a typical 'hard' base, was expected to form strong complexes with a 'hard' acid like W^{6+} (Watson 1976; Ryerson and Hess 1980; Webster et al. 1997). According to London et al. (1993), phosphorus partitions strongly in favor of a silicate melt phase, so the low partition coefficient of W between the P-rich melt and aqueous fluid wss expected. However, Keppler (1994) found that the phosphorus content of a coexisting aqueous fluid increases with the total phosphorus content in the melt and with pressure. This result may account for the fact that the vapor/melt partition coefficients of tungsten increase with

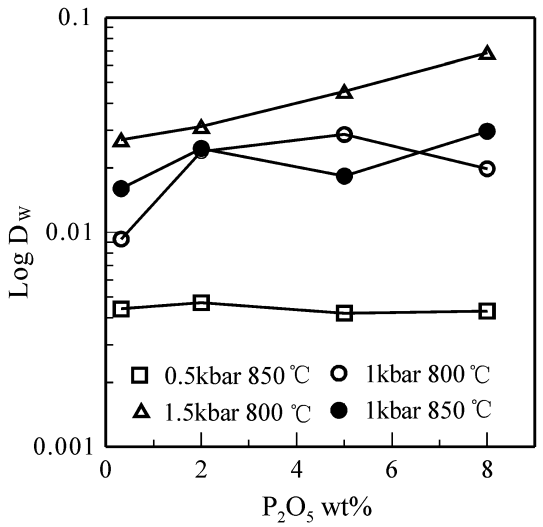

Fig. 1 Partition coefficients of tungsten between aqueous fluid and melt

increasing P_2O_5 wt% in the melt and increasing pressure (Fig. 1).

The distribution of tungsten between granite melt and the coexisting fluid has been studied extensively (Manning and Henderson 1984; Keppler and Wyllie 1991; Chen and Peng 1994; Zhao et al. 1996; Bai and Koster van Groos 1999). Except for the results of Manning and Henderson (1984), previous studies showed that the capacity of tungsten to dissolve in an aqueous fluid decreases in the following sequence of anions present: Cl, pure $H_2O > CO_2 > F > P$. Our data for W contrast with the results

of Manning and Henderson (1984), who found that W fractionates toward the fluid in a P-bearing system ($D_W = 2.0–2.7$ at 800 °C and 100 MPa). Though our experiments do not provide any information on the oxidation state of tungsten in te melt and the fluid, we assume fO_2 to be with in 2 log units of the NNO buffer (see experimental section). Under these fO_2 conditions, the oxidation state of tungsten is +6. Furthermore, Bai and Koster van Groos (1999) and Chen and Peng (1994) considered that the presence of a small amount of reduced tungsten does not significantly affect its distribution behavior. The differences of D_W in our work and in the study of Manning and Henderson (1984) are unlikely to be the result of differences in fO_2, but are more likely to be from differences in fluid composition. The addition of large amounts of Na_3PO_4 made the bulk of their composition peralkaline, and increased the pH of the solution (Urabe 1985). Furthermore, the tungsten concentration (1 wt% W) used by Manning and Henderson (1984) was so high that W could have deviated from Henry's law distribution. In contrast, the

Table 3 Partition coefficient of W between aqueous fluid and melt

Run no	T (°C)	P (Mpa)	C_{fluid} (ppm)	C_{melt} (ppm)	D
P0T-30-1	850	50	1.74	397.22	0.0044
P0T-27-7	800	100	3.67	394.78	0.0093
P0T-26-7	850	100	6.39	400.42	0.0160
P0T-28-3	800	150	10.91	403.51	0.0270
P2T-30-7	850	50	2.28	481.35	0.0047
P2T-24-8	800	100	10.92	458.99	0.0238
P2T-23-8	850	100	11.60	471.24	0.0246
P2T-28-4	800	150	14.65	469.07	0.0312
P5T-29-1	850	50	2.10	506.35	0.0042
P5T-24-7	800	100	13.41	469.25	0.0286
P5T-26-4	850	100	8.60	471.11	0.0183
P5T-28-7	800	150	21.20	467.31	0.0454
P8T-30-8	850	50	0.70	163.34	0.0043
P8T-26-3	800	100	9.70	489.31	0.0198
P8T-26-8	850	100	14.41	486.50	0.0296
P8T-28-8	800	150	32.63	475.29	0.0687

Table 4 Partition coefficients of Niobium between aqueous fluid and melt

Run no	T (°C)	P (kbar)	C_{fluid} (ppm)	C_{melt} (ppm)	$D_{fluid/melt}$
P0T-30-1	850	50	0.031	207.43	0.00015
P0T-27-7	800	100	0.022	203.57	0.00011
P0T-26-7	850	100	0.046	208.64	0.00022
P0T-28-3	800	150	0.149	208.51	0.00071
P2T-30-7	850	50	0.016	236.15	0.00007
P2T-24-8	800	100	0.085	227.01	0.00037
P2T-23-8	850	100	0.092	222.33	0.00041
P2T-28-4	800	150	0.238	224.66	0.00106
P5T-29-1	850	50	0.017	276.50	0.00006
P5T-24-7	800	100	0.073	260.76	0.00028
P5T-26-4	850	100	0.088	265.88	0.00033
P5T-28-7	800	150	0.128	259.62	0.00049
P8T-30-8	850	50	0.017	132.54	0.00013
P8T-26-3	800	100	0.042	397.60	0.00010
P8T-26-8	850	100	0.220	390.06	0.00056
P8T-28-8	800	150	0.473	367.58	0.00129

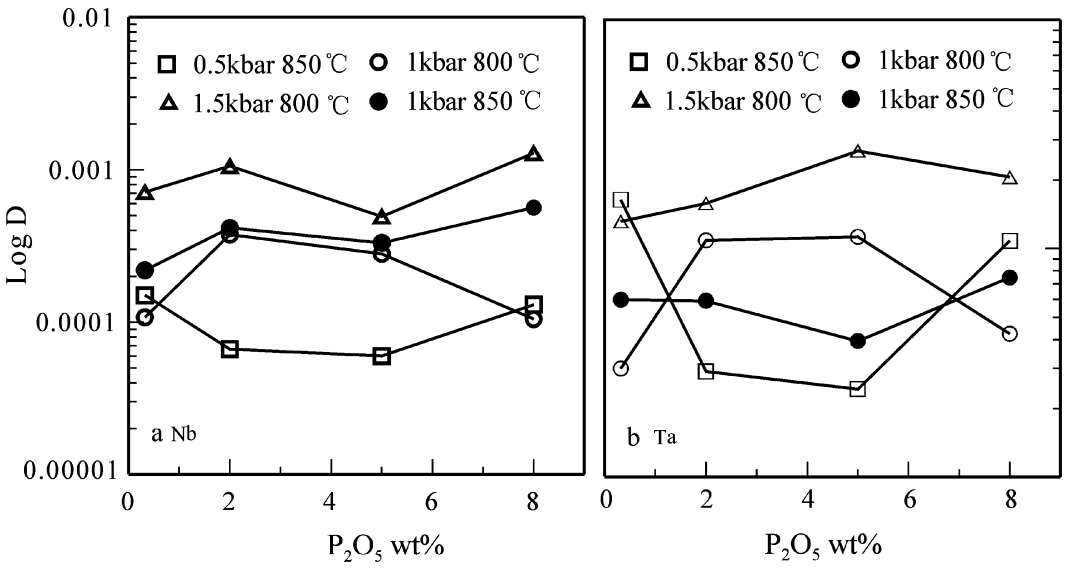

Fig. 2 Partition coefficients of Niobium and Tantalum between aqueous fluid and melt

Table 5 Partition coefficients of Tantalum between aqueous fluid and melt

Run no	T (°C)	P (kbar)	C_{fluid} (ppm)	C_{melt} (ppm)	$D_{fluid/melt}$
P0T-30-1	850	50	0.029	179.30	0.00016
P0T-27-7	800	100	0.005	170.72	0.00003
P0T-26-7	850	100	0.011	181.11	0.00006
P0T-28-3	800	150	0.024	181.08	0.00013
P2T-30-7	850	50	0.006	216.94	0.00003
P2T-24-8	800	100	0.023	208.19	0.00011
P2T-23-8	850	100	0.012	207.00	0.00006
P2T-28-4	800	150	0.034	217.16	0.00016
P5T-29-1	850	50	0.005	196.54	0.00002
P5T-24-7	800	100	0.021	185.76	0.00011
P5T-26-4	850	100	0.008	194.85	0.00004
P5T-28-7	800	150	0.054	203.31	0.00027
P8T-30-8	850	50	0.008	74.63	0.00011
P8T-26-3	800	100	0.009	223.88	0.00004
P8T-26-8	850	100	0.017	222.07	0.00007
P8T-28-8	800	150	0.043	209.78	0.00021

concentrations of W used in our experiments were more geologically relevant.

3.3 Niobium and tantalum

The data for D_{Nb} and D_{Ta} are shown in Fig. 2, Tables 4 and 5. The distribution behaviors of niobium and tantalum are very similar in our experiments. The partition coefficients of the two elements are very low ($D_{Nb} = 0.00005–0.01$ and $D_{Ta} = 0.00003–0.002$). A change in starting P_2O_5 of the glasses contents between 1.91 and 4.83 wt% has no significant effect on D_{Nb} and D_{Ta}. But as the pressure increases, both D_{Nb} and D_{Ta} increase.

In previous studies, D_{Nb} varied 1–3 orders of magnitude. Webster et al. (1989) found D_{Nb} to be affected by pressure, temperature and fluid composition for F-enriched topaz rhyolite melt. At pressure = 4.0 kbar, Nb partitions into the melt, with the partitioning being apparently independent of temperature. As the pressure decreases, Nb partitions in favor of the fluid and D_{Nb} increase with temperature. As the mole fraction of water in the fluid increases, Nb partitions increasingly in favor of the fluid. Our D_{Nb} is similar to the values found by London et al. (1988) and Zhao et al. (1996) (0–0.1 and 0.0019–0.081 respectively), although their D_{Nb} is higher than ours. Zhao et al. (1996) determined $D_{Ta} = 0.0023–0.089$. The differences between the results we obtained and previous studies are likely mainly attributed to the difference in fluid composition and melt.

4 Conclusions

Relative to the coexisting aqueous fluid, W, Nb and Ta partition in favor of P-rich peraluminous granitic melt at 800–850 °C and 50–150 MPa. The ranges of the fluid/melt partition coefficients of W, Nb and Ta are: 0.003–0.07, 0.00005–0.001, 0.00003–0.0002, respectively. D_W, D_{Nb}, and D_{Ta} are all affected by pressure, but there is no evidence of an effect of P_2O_5 on these elements, except for W.

The D_W is less than 0.01; therefore it is difficult to derive a W-enriched fluid from a P-rich peraluminous melt system, especially when phosphorus is the only complexing agent. Our results also show that Nb and Ta tend to distribute in the melt when it is in the magmatic-hydrothermal stage. In the late period of crystallization of magma, Nb and Ta will form discrete independent minerals like tantalite and columbite.

Acknowledgments This research project is supported by the Chinese National Natural Science Foundation (Project No. 40273030) and the Chinese Academy of Sciences through an innovation project (Project No. KZCX3-SW-124).

References

Bai T, van Koster Groos AF (1999) The distribution of Na, K, Rb, Sr, Al, Ge, Cu, W, Mo, La, and Ce between granitic melts and coexisting aqueous fluids[J]. Geochim et Cosmochim Acta 63:1117–1131

Chen ZL, Peng SL (1994) The experimental results of W and Sn partitioning between fluid and melt and their significance for the origin of W and Sn ore deposits[J]. Geol Rev 40(3):274–282 (in Chinese with English abstract)

Chou IM (1987) Oxygen buffer and hydrogen sensor technique at elevated pressures and temperatures. In: Barnes HL, Ulmer GC (eds) Hydrothermal experiments techniques[M]. Wiley, New York

Dingwell DB, Knoche R, Webb SL (1993) The effect of P_2O_5 on the viscosity of haplogranitic liquid. Eur J Mineral 5:133–140

Gao S, Liu XM, Yuan HL, Hattendorf B, Gunther D, Chen L, Hu SH (2002) Determination of forty two major and trace elements in USGS and NIST SRM glasses by laser ablation-inductively coupled plasma-mass spectrometry[J]. ostand Newsl: J Geostand and Geoanal 26:181–196

Holtz F, Dingwell DB, Behrens H (1993) Effects of F, B_2O_3 and P_2O_5 on the solubility of water in haplogranite melts compared to natural silicate melts[J]. Contrib Mineral Petrol 113:492–501

Huang XL, Wang RC, Chen XM, Hu H, Liu CS (2002) Vertical variations in the mineralogy of the Yichun Topaz-Lepidolite granite, Jiangxi Province, southern China[J]. Can Mineral 40(4):1047–1068

Keppler H (1994) Partitioning of phosphorus between melt and fluid in the system haplogranite-H_2O-P_2O_5[J]. Chem Geol 117:345–353

Keppler H, Wyllie PJ (1991) Partitioning of Cu, Sn, Mo, W, U, and Th between melt and aqueous fluid in the systems haplogranite-H_2O-HCl and haplogranite-H_2O-HF[J]. Contrib Mineral Petrol 109:139–150

Lentz DR (1997) Phosphorus-enriched, S-type Middle River Rhyolite, Tetagouche Group, northeastern New Brunswick; petrogenetic implications[J]. Can Mineral 35:673–690

Li G, Hua R, Li X, Wei X, H xiaoe, Hu D, Zhang W, Wang X (2010) Discovery and geological significance of triplite in Baxiannao tungsten deposit, southern Jiangxi Province, China[J]. Acta Mineral Sin 30(3):273–277

London D (1987) Internal differentiation of rare-element pegmatites: effects of boron, phosphorus, and fluorine[J]. Geochim Cosmochim Acta 51:403–420

London D (1998) Phosphorus-rich peraluminous granites[J]. Acta Univ Carol-Geol 42:64–68

London D, Hervig RL, Morgan GB (1988) Melt-vapor solubilities and elemental partitioning in peraluminous granite-pegmatite systems: experimental results with Macusani glass at 200 MPa[J]. Contrib Mineral Petrol 99:360–373

London D, Morgan VI GB, Richard LH (1989) Vapor-undersaturated experiments with Macusani glass+ H_2O at 200 Mpa, and the internal differentiation of granitic pegmatites[J]. Contrib Miner Petrol 102:1–17

London D, Morgan VIGB, Babb HA, Loomis JL (1993) Behavior and effects of phosphorus in the system Na_2O–K_2O–Al_2O_3–SiO_2–P_2O_5–H_2O at 200 MPa(H_2O)[J]. Contrib Mineral Petrol 113:450–465

London D, Wolf MB, Morgan VIGB, Garrido MG (1999) Experimental Silicate-Phosphate equilibria in peraluminous granitic magmas, with a case study of the Alburquerque batholith at Tres Arroyos, Badajoz, Spain[J]. J Petrol 40(1):215–240

Manning D, Henderson P (1984) The behaviour of tungsten in granitic melt-vapour systems[J]. Contrib Mineral Petrol 86:286–293

Morgan VIGB, London D (1996) Optimizing the electron microprobe analysis of hydrous alkali aluminosilicate glasses[J]. Am Mineral 81:1176–1185

Morgan VIGB, London D (2005) Effect of current density on the electron microprobe analysis of alkali aluminosilicate glasses[J]. Am Mineral 90:1131–1138

Raimbault L, Burol L (1998) The Richemont rhyolite dike, massif central, France: a subvocanic equivalent of rare-metal granite[J]. Can Mineral 36:265–282

Raimbault L, Cuney M, Azencott C, Duthou JL, Joron JL (1995) Geochemical evidence for a multistage magmatic genesis of Ta-Sn-Li mineralization in the granite at Beauvoir, French Massif Central[J]. Econ Geol 90:548–576

Ryerson FJ, Hess PC (1980) The role of P_2O_5 in silicate melts[J]. Geochim Cosmochim Acta 44:611–624

Simon AC, Frank MR, Pettke T, Candela PA, Piccoli PM, Heinrich CA (2005) Gold partitioning in melt-vapor-brine systems[J]. Geochim Cosmochim Acta 69:3321–3335

Tang Y, Zhang H, Liu C-Q, Rao B (2009) Experimental study of effect of phosphorus on liquidus temperature of peraluminous magmatic system[J]. Geochimica 38(1):37–42 (in Chinese with English abstract)

Toplis MJ, Dingwell DB (1996) The variable influence of P_2O_5 on the viscosity of melts of differing alkali/aluminium ratio: implications for the structural role of phosphorus in silicate melts[J]. Geochim Cosmochim Acta 60:4107–4121

Urabe T (1985) Aluminous granite as a source magma of hydrothermal ore deposits; an experimental study[J]. Econ Geol 80:148–157

Watson EB (1976) Two-liquid partition coefficients: experimental data and geochemical implications[J]. Contrib Mineral Petrol 56:119–134

Webster JD (1990) Partitioning of F between H_2O and CO_2 fluids and topaz rhyolite melt. Contrib Mineral Petrol 104:424–438

Webster JD, Holloway JR, Hervig R (1989) Partitioning of lithophile trace elements between H_2O and H_2O+ CO_2 fluids and topaz rhyolite melt[J]. Econ Geol 84(1):116–134

Webster JD, Thomas R, Rhede D, Forster H-J, Seltmann R (1997) Melt inclusions in quartz from an evolved peraluminous pegmatite: geochemical evidence for strong tin enrichment in fluorine-rich and phosphorus-rich residual liquids[J]. Geochim Cosmochim Acta 61(13):2589–2604

Wyllie PJ, Tuttle OF (1964) Experimental investigation of silicate systems containing two volatile components: part III. the effets of SO_3, P_2O_5, HCl and Li_2O in addition to H_2O, on the melting temperatures of Albite and granite[J]. Am J Sci 3:930–939

Yang YQ, Wang WY, Ni YX, Chen CH, Zhu JH (1994) Phosphate minerals and Their Geochemical Evolution of granitic pegmatite in Nanping, Fujian Province[J]. Geol Fujian 13(4):215–226 (in Chinese with English abstract)

Zhang H (2001) The geochemical behaviors and mechanisms of incompatible trace elements in the magmatic-hydrothermal transition system: a case study of Altay No. 3 pegmatite, Xinjiang. Dissertation for the Doctoral Degree, Guiyang: Institute of Geochemistry, Chinese Academy of Sciences (in Chinese with English abstract)

Zhao JS, Zhao B, Rao B (1996) A preliminary experimental study on mineralization of Nb, Ta and W[J]. Gochimica 25(3):286–295 (in Chinese with English abstract)